

Electroreflectance of GaSb from 0.6 to 26 eV

D. E. Aspnes

Bell Laboratories, Murray Hill, New Jersey 07974

C. G. Olson and D. W. Lynch

Ames Laboratory, Energy Research and Development Administration and Department of Physics, Iowa State University,

Ames, Iowa 50010

(Received 16 March 1976)

Schottky barrier electroreflectance spectra are reported for GaSb from 0.6 to 26 eV. Accurate energies are determined for a number of critical points between the sp^3 and Ga-3*d* valence bands and the conduction bands. The energy of X_7^V is shown to lie at least 3 eV below Γ_8^V . This is below the value obtained from local pseudopotential calculations and the x-ray photoemission assignments, but follows a trend previously established by nonlocal pseudopotential calculations for Ge and GaAs. The Ga 3*d*- X_6^C exciton binding energy is of the order of 100 meV.

I. INTRODUCTION

GaSb is an interesting material with respect to solid-state spectroscopy and energy-band theory. The lack of inversion symmetry leads to a much richer optical spectrum than for its closest group-IV counterpart Ge. Because the spin-orbit splitting of Sb is large, the critical-point structures tend to be spread out so that the major singularities are observed with less overlap than with other members of the III-V family. It is therefore possible to obtain a number of critical-point energies to high accuracy.

GaSb should consequently provide an excellent test of recently developed nonlocal pseudopotential methods,¹⁻⁵ which have calculated very successfully the energy bands of Ge and GaAs over a wide range of photon energies. Of particular interest will be the capability of these techniques to deal with exchange, correlation, and relativistic effects which are substantially more important in GaSb than in other materials to which they have been applied.

The primary purpose of this work is to obtain accurate energies for interband critical points in GaSb. Critical points measured include not only those from the sp^3 valence bands, but also from the Ga 3*d* core levels located approximately 19 eV below the top of the sp^3 valence bands. The Schottky barrier electroreflectance (ER) method^{6,7} was used. Its sensitivity enabled us to resolve some new critical-point features. The identification of several of these cannot be made with the presently available information, which emphasizes further the need for an accurate energy-band calculation.

The outline of the paper is as follows: Experimental details are summarized in Sec. II. Results are discussed in Sec. III according to major

critical-point groupings, with the critical-point energies summarized in Table I and the spin-orbit splittings in Table II. In Sec. IV, we compare briefly our results with the probable best⁸ of several⁹⁻¹² currently available band-structure calculations for GaSb. Spin-orbit splittings are also compared to theoretical calculations.¹³ We discuss the interesting question of the energies of the X_6^C and X_7^C points. By comparing our core-level measurements with x-ray photoemission (XPS) measurements¹⁴ locating Ga 3*d*^V and pressure measurements¹⁵ locating X_6^C , we obtain a binding energy of 90 meV for the Ga 3*d*^V- X_6^C exciton.

II. EXPERIMENTAL

All measurements reported here were obtained on a bromine-methanol polished {111} B(Sb) surface on an *n*-type single crystal of GaSb of carrier concentration $N_D = 1.1 \times 10^{17} \text{ cm}^{-3}$. To remove any possibility of residual damage, the surface was anodized to form an 0.3- μm oxide layer, which was then stripped in HCl.¹⁶ A 40- \AA film of Ni was evaporated as described elsewhere^{7,17} to form a Schottky barrier on this surface. To reduce oxidation effects in the Ni film, the sample was stored under vacuum prior to measurement in the vacuum uv except for one evaluation spectrum measured from 1.8–5.5 eV just after evaporation. The evaluation spectrum was the same as later spectra taken under the same conditions, showing that oxidation effects were negligible.

Measurements in the 0.6–6.2-eV spectral range were performed using standard quartz-optic techniques with equipment already described.⁷ A PbS cell, a Si photodetector, and an EMI 9556QB photomultiplier were used for the spectral ranges 0.6–1.2, 1.2–1.8, and 1.7–6.2 eV, respectively.

The sample temperature for these measurements was of the order of 10 K (liquid He cold finger). The flux was nominally unpolarized. The monochromator was calibrated with a Hg spectral line source.

Measurements in the 5.5–27-eV spectral range were performed using the high-energy photon source of the Synchrotron Radiation Center of the Physical Sciences Laboratory of the University of Wisconsin. All measurements were performed at a sample temperature of approximately 110 K (liquid N₂ cold finger), using techniques and apparatus that also have been described previously.^{18–20} Predominantly *p*-polarized flux was reflected at a 60° angle of incidence to maximize²¹ the signal-to-noise ratio in this spectral region.

All spectra were measured using 103-Hz square-wave modulation from a typical value of +0.3 V in the forward direction to various reverse voltages up to the breakdown limit at –1.8 V. The maximum attainable surface field \mathcal{E}_s at breakdown was calculated from $N_D = 1.1 \times 10^{17} \text{ cm}^{-3}$ and²² $\epsilon_0 = 15.7$ to be 230 kV/cm. To check independently this value, \mathcal{E}_s was also calculated from the Franz-Keldysh oscillations observed at maximum modulation for the E_0 transition, using the asymptotic theory²³ to evaluate $\hbar\Omega$ from the energies at which the oscillations were tangent to their envelope.^{7,24} Using the heavy-hole reduced mass $\mu_{\text{hh}} = 0.041m_e$,²⁵ whose contribution to Schottky barrier ER dominates that of the light hole unless separated explicitly,^{24,26} we calculate $\mathcal{E}_s = 230 \text{ kV/cm}$. This value, in excellent agreement with that calculated from the barrier potential and N_D , confirms the value of N_D in the barrier region and justifies the use of the barrier equation to calculate the surface field for other modulation levels.

Since the determination of the critical-point energies was the main objective of this work, we have not analyzed line shapes in detail. Due to the relatively large doping, it was not possible to achieve simultaneously the low-field limit and the uniform-field condition for the E_0 structure for any value of surface field.²⁷ The E_0 transition clearly exhibited a line-shape evolution²⁸ toward the uniform-field limit with increasing reverse bias, as expected in the Schottky barrier configuration. Modulation conditions for spectra for critical-point energy analysis purposes were chosen to favor the low-field condition at the expense of field uniformity.

III. RESULTS AND DISCUSSION

A. $E_0, E_0 + \Delta_0$ transitions

ER spectra for the E_0 and $E_0 + \Delta_0$ transitions, taken with $\mathcal{E}_s = 90 \text{ kV cm}^{-1}$ (+0.30–0.00-V modula-

tion), are shown in Fig. 1. Energies of 0.822 ± 0.005 and $1.575 \pm 0.005 \text{ eV}$ were determined for the E_0 and $E_0 + \Delta_0$ critical points, respectively, and are indicated by lines in the figure. These energies were obtained by fitting to the experimental curve over a limited energy range containing the structure a theoretical low-field two-dimensional M_0 critical-point ER function²⁹

$$\Delta R/R = \text{Re}[Ce^{i\theta}(E - E_g + i\Gamma)^{-3}] + b, \quad (1)$$

where C , θ , E_g , and Γ are adjustable parameters and the baseline b is chosen to account for zero offset (if any). The curve-fit energy for E_0 was corrected by adding the exciton rydberg of 2 meV as calculated from the parameters of this material.²⁵ The fitting procedure is an extension of the three-point method³⁰ that is better suited to digital computation and provides better averaging by using more of the line shape. The spin-orbit splitting calculated from these data is $\Delta_0 = 753 \pm 5 \text{ meV}$.

These results are in essential agreement with previous absorption³¹ and stress-modulated magnetorelectance^{32–34} data on *p*-type samples. The most reliable values of the E_0 critical-point energy and the spin-orbit splitting Δ_0 are 0.8102 eV,³³ and 749 meV,³⁴ respectively. Our larger values can be understood as arising from degeneracy effects. Indeed, assuming an ideal parabolic band structure with $m_c^* = 0.042m_e$,²⁵ and $N_D = 1.1 \times 10^{17} \text{ cm}^{-3}$, we calculate $E_F - E_C = 19 \text{ meV}$. Our observed difference of 12 meV for E_0 is less, possibly for a number of reasons including carrier freezeout and exchange effects which depress the interband energy separation with increasing impurity concentration.³⁵ The discrepancy between spin-orbit splittings is less than 12 meV since it concerns

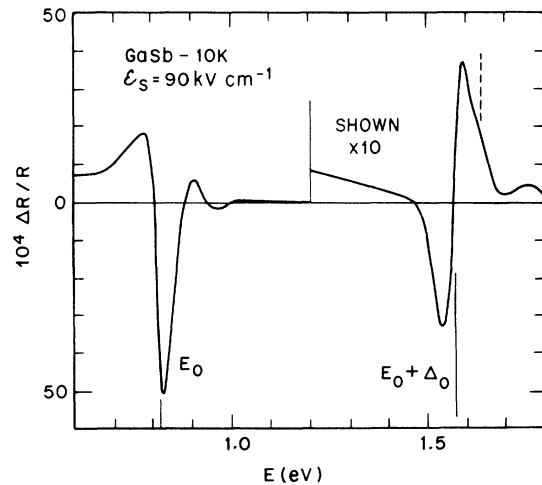


FIG. 1. Schottky barrier ER spectrum of the E_0 and $E_0 + \Delta_0$ transitions of GaSb. The location of the anomalous $E_0 + \Delta_0$ structure is indicated by the dashed line.

only the difference in energy between the spin-orbit split Γ_7^V valence band and the heavy-hole Γ_8^V valence band. As in Ge,²⁶ it appears that the light-hole Γ_8^V band does not contribute substantially to the total E_0 structure, as expected from density-of-states considerations.

Two line-shape peculiarities in these structures are worth mentioning: the significant difference between the E_0 and $E_0 + \Delta_0$ line shapes, and the appearance of an anomalous structure (weak in Fig. 1) about 60 meV above $E_0 + \Delta_0$. This structure is strongly dependent on the value of the voltage for the positive half of the modulation cycle. The main $E_0 + \Delta_0$ structure has the general appearance of a M_0 critical point, with small asymmetry corrections³⁶ from the optical properties of the Ni overlayer, field inhomogeneity effects,²⁸ and electron-hole correlation effects.³⁷ Since the transition type and the optical properties of GaSb and Ni at the E_0 threshold are nominally the same, the substantially different line shape for E_0 is at first sight surprising. The difference is probably due to the essential singularity of the light- and heavy-hole valence bands for E_0 , and more accurate line-shape calculations^{38,39} for these singularities may resolve this problem.

The anomalous structure in $E_0 + \Delta_0$ is weak for modulation from +0.30 V, but it dominates the line shape for modulation from 0.00 V. It is seen at no other critical point in GaSb. We believe that it is related to a similar effect seen in InSb and InAs by Bottka *et al.*,⁴⁰ which has been interpreted tentatively in terms of band-population effects.⁴¹⁻⁴³

B. $E_1, E_1 + \Delta_1$ transitions

The E_1 and $E_1 + \Delta_1$ line shapes shown in Fig. 2 are quite similar to those obtained in Schottky barrier ER measurements on other semiconductors.^{7,26} We find by curve fitting the critical-point energies 2.195 ± 0.010 and 2.625 ± 0.010 eV for the E_1 and $E_1 + \Delta_1$ critical points, respectively. The spin-orbit splitting is $\Delta_1 = 430 \pm 10$ meV. Stress measurements^{44,45} place these transitions along Λ or L , in agreement with similar materials; a line-shape analysis of heterojunction ER spectra⁴⁶ shows that M_1 critical points are responsible for the structures. The Δ_1 value is about 15% less than that predicted by the simple two-thirds rule,⁴⁷ due to the influence of neighboring bands.¹³

Our energy values show some differences with respect to wavelength modulation results,^{48,49} which place the critical-point energies 30–90 meV lower as a result of the greater uncertainty in interpreting the features of the less-well-structured first-derivative line shapes. Spin-orbit-splitting values of 445,⁴⁴ 442,⁴⁸ and 438 meV,⁴⁹

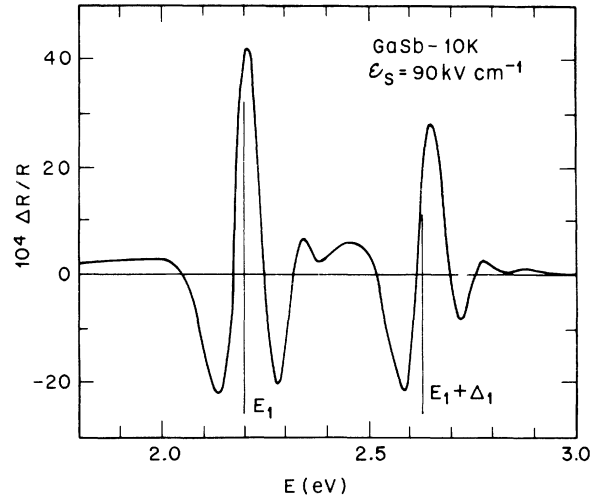


FIG. 2. Schottky barrier ER spectrum of the E_1 and $E_1 + \Delta_1$ transitions of GaSb.

calculated from the first-derivative results, are closer to our value of 430 ± 10 meV. The better agreement for Δ_1 is not surprising since interpretational ambiguities are reduced for difference calculations.

C. E'_0 triplet

The earliest interpretation of the weak E'_0 triplet structures as originating at^{50,51} Γ was later questioned in GaSb in favor of a Δ assignment.^{48,49} But symmetry analysis^{52,53} of the E'_0 features in Ge identified the critical-point symmetry as Γ , and this was confirmed later by accurate critical-point energy measurements which showed for both Ge,⁶ and GaAs,⁷ an energy separation of the second and third structures equal to the spin-orbit splitting of the top of the valence band.

Our values for the three E'_0 critical-point energies are 3.191 ± 0.005 , 3.404 ± 0.010 , and 4.160 ± 0.010 eV. These were obtained by curve fitting to line shapes taken with $\mathcal{E}_s = 90$ kV cm⁻¹, which are shown in Fig. 3. The energy obtained for the highest-energy member is in principle less accurately determined due to its overlap with the X and E_2 structures, but this uncertainty was minimized by calculating a second derivative of the ER line shape (see Fig. 5 and associated discussion). The calculated spin-orbit splittings are $\Delta'_0 = 213 \pm 10$ meV and $\Delta''_0 = 756 \pm 15$ meV.

The spin-orbit splittings are in good agreement with the values 215 ± 5 and 745 ± 5 meV obtained in metal-oxide-semiconductor (MOS) measurements on similar n -type GaSb by Parsons and Piller,⁵⁴ although their critical-point energies are 30–40 meV low due to their (incorrect) assignment of the

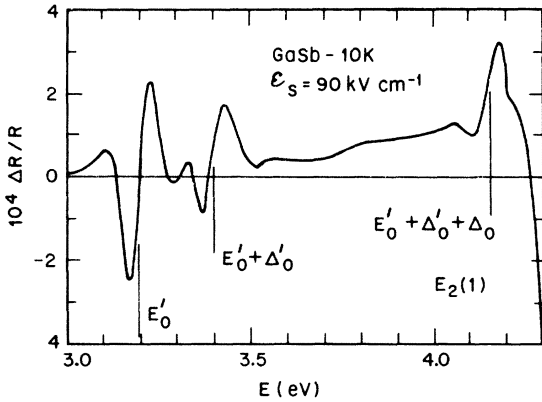


FIG. 3. Schottky barrier ER spectrum of the E'_0 triplet of GaSb.

critical-point energy to the positive peak on the ER spectrum. The observation of the valence-band spin-orbit splitting value near $\Delta_0 = 749$ meV for Δ_0'' confirms the assignment of Γ symmetry for GaSb.^{50, 51, 54} We believe that our spin-orbit-splitting energies are more reliable than those of Parsons and Piller because their values were obtained from peaks alone, and consequently are influenced by changes in lifetime broadening, which acts to spread the structures differently.

The near degeneracy of Γ and Δ critical points observed for E'_0 in⁷ GaAs appears to be missing in GaSb, although the line shape for $E'_0 + \Delta'_0$ indicates that some extra critical-point structure may be present. But this is not surprising since both Γ_8^V and Γ_8^C are essential degeneracies.

As with GaAs,⁷ highly structured Schottky barrier ER spectra are obtained for GaSb in the vicinity of the E_2 peak. A typical spectrum obtained at $\mathcal{E}_s = 90$ kV cm⁻¹ is shown in Fig. 4. In order to better resolve weak transitions appearing only as shoulders of stronger transitions, a higher-field ER spectrum ($\mathcal{E}_s = 240$ kV cm⁻¹) was differentiated numerically twice with respect to energy. The result is shown in Fig. 5.

We consider first the dominant spectral features seen in Fig. 4. The $E'_0 + \Delta'_0 + \Delta_0''$ structure at 4.160 eV has already been discussed. The large feature near 4.40 eV labeled $E_2(1), E_2(2)$ is a common feature of these materials. But for GaSb, it appears to be split into two components separated by an energy difference of the order of 30–40 meV, obtained by inspection of the anomalous width of the lower-energy half of the line shape. This splitting is too small to be ascribed to the spin-orbit interaction, and probably is a result of two critical points lying very close in both energy and wave vector. Further evidence for proximity follows from the decrease in apparent splitting with in-

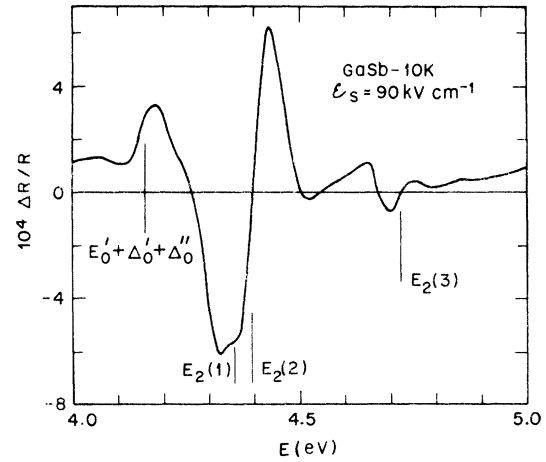


FIG. 4. Schottky barrier ER spectrum of the E'_2 complex of GaSb.

creasing field.⁷ Detailed energy-band calculations for³ Ge locate the critical point(s) giving rise to the E_2 structure in Ge near $(\frac{1}{4}, \frac{1}{4}, \frac{1}{4})$. A similar location is probable for GaSb. The peak in reflectance occurs at 4.35 eV,⁴⁸ slightly lower in energy than E_2 . The location and symmetry of the third large transition, $E_2(3)$ at 4.72 ± 0.05 eV in Fig. 4, is not known.

Several weaker structures are evident in the numerically differentiated spectrum of Fig. 5. Similar transitions near E_2 in GaAs were identified by polarization measurements on a $\{110\}$ surface and by the observation of a doublet-doublet energy separation as originating from critical points near X .⁷ No obvious doublet-doublet pattern is expected here because the calculated spin-orbit splitting of the valence band, $\Delta_2 = X_6^V - X_7^V$, is 0.24 eV,¹³ about the same as that expected for the antisymmetric

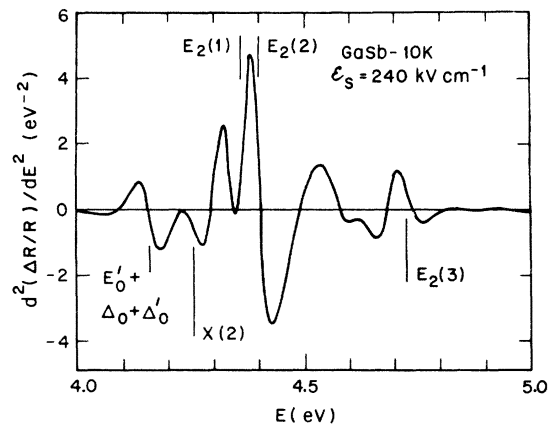


FIG. 5. Second energy derivative of a higher-field ER spectrum of the E_2 complex of GaSb.

potential splitting of X_6^C and X_7^C .⁵⁵ The X transitions should therefore spread over a range of the order of $\frac{1}{2}$ eV.

Since all four X transitions should possess reasonable and nearly equal oscillator strengths, it is clear from Figs. 3–5 that the lowest X transition ($X_7^V \rightarrow X_6^C$) must lie at least as high as 4.16 eV, the energy of $E'_0 + \Delta'_0 + \Delta_0$, since there is no evidence of any critical-point structure below this or above $E'_0 + \Delta'_0$, a range of over 0.5 eV. For if $X_7^V \rightarrow X_6^C$ were to lie at or near $E'_0 + \Delta'_0$ at 3.5 eV, then at least one of the remaining X transitions should appear in the 3.55–4.05-eV range. This is not observed.

Due to the presence of the E_2 transitions, there is no obvious way to assign structures in the vicinity of E_2 to the X quadruplet. For want of a better choice, we assign the 4.26-eV structure in Fig. 5 to $X_7^V \rightarrow X_6^C$. Although a number of possibilities exist for the remaining assignments, none are particularly satisfactory because of unacceptable variations in apparent oscillator strength or unrealistic energy separations. A further discussion of the energies of the critical points at X , with regard to core-level ER and x-ray photoemission (XPS) data¹⁴ is given in Sec. IV.

D. E'_1 complex

By contrast to GaAs,⁷ the E'_1 complex lies in the quartz-optics range. Typical spectra, taken at a surface field of 90 kV cm^{-1} , are shown in Fig. 6.

The dominant features here include the main peak with critical-point energy at 5.59 ± 0.03 eV, and the higher-energy component at 6.04 ± 0.03 eV. The energy separation of 450 ± 30 meV is in good agreement with the spin-orbit splitting, $\Delta_1 = 430$

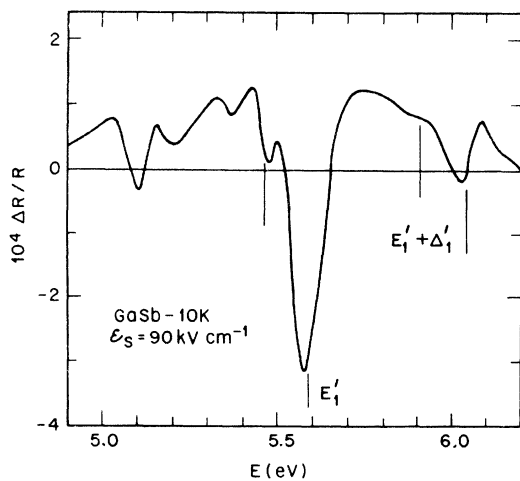


FIG. 6. Schottky barrier ER spectrum of the E'_1 complex of GaSb.

± 10 meV, of the valence bands at Λ . This agreement, which is also nearly exact in α -Sn,⁵⁶ has been used to support a Λ - or L -symmetry origin for these critical points. But band-structure calculations⁵⁷ for GaP and GaAs, and the observation of a substantial difference between these spin-orbit splittings for Ge,²⁶ and other semiconductors,^{20, 58} has indicated that these critical points, if indeed near Λ , are off the symmetry axis for many of these materials.⁵⁹ This may not be the case for GaSb.

Several weak structures also occur in the 5.1–5.6-eV range. The two structures at 5.37 and 5.46 eV are remarkable for their sharpness. It is possible to correlate the 5.46-eV structure and the dip at 5.9 eV with transitions to the $L_{4,5}^C$ band since both are about 130 meV below the nominally E'_1 and $E'_1 + \Delta'_1$ transitions and their strengths are in proportion to the main structures. Therefore 130 meV becomes the spin-orbit splitting between $L_{4,5}^C$ and L_6^C , which is in good agreement with theory.¹³ But it is not clear why the oscillator strengths should be so weak for the transitions terminating on the $L_{4,5}^C$ band.

E. E''_0 range

ER spectra in the vacuum uv spectral region from 6 to 12 eV are shown in Fig. 7. The highest-energy component of the E'_1 complex in Fig. 6 appears at the far left and indicates the relative magnitude of the remaining structures. These spectra are considerably weaker than similar data for GaAs and²⁰ GaP owing to the difficulty of obtaining high surface fields in GaSb, a consequence of its relatively small band gap.

The only unambiguous structure in this range is E''_0 ($\Gamma_8^V \rightarrow \Gamma_{12}^C$) with a critical-point energy of 7.9 ± 0.1 eV, which can be identified by its line-shape

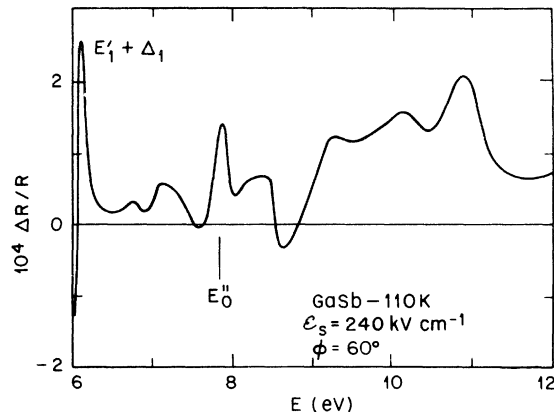


FIG. 7. Schottky barrier ER spectrum of the 6–12-eV region of GaSb.

similarity to the corresponding structure in GaP, at 9.38 ± 0.1 eV in that material. Thus the conduction-band d -like bonding levels lie substantially lower in GaSb. The spin-orbit-split structure expected from Γ_7^V is absent, probably because of the small density of states from the small spin-orbit-split hole mass.

The remaining structures in this energy range are relatively broad, and probably occur in regions of low symmetry.

No structures were observed in the energy range from 12 eV to the onset of core-level transitions near 20 eV. This was due to the facts that the structure is broad even under the best of conditions, and that the fields obtained even at maximum possible modulation were relatively low.

F. Core-level transitions

ER spectra for transitions between the Ga $3d$ core levels and the sp^3 conduction band are shown in Figs. 8 and 9. These data were obtained with a spectral resolution of 150 meV. Figure 9 shows in expanded form the critical-point structures between the spin-orbit-split $j = \frac{3}{2}$ and $j = \frac{5}{2}$ core levels, and the X_6^C conduction-band relative minimum. No evidence is seen for a critical-point structure between the core levels and the Γ_6^C conduction-band absolute minimum, but this is expected from matrix element considerations.²⁰

In general, the core-level spectra of GaSb are more highly structured than those of GaP and GaAs, with more overlap between structures. This is not surprising in view of the downshift of the energies of all features of the sp^3 valence-conduction-band critical-point spectrum, which places more local conduction-band extrema within the ex-

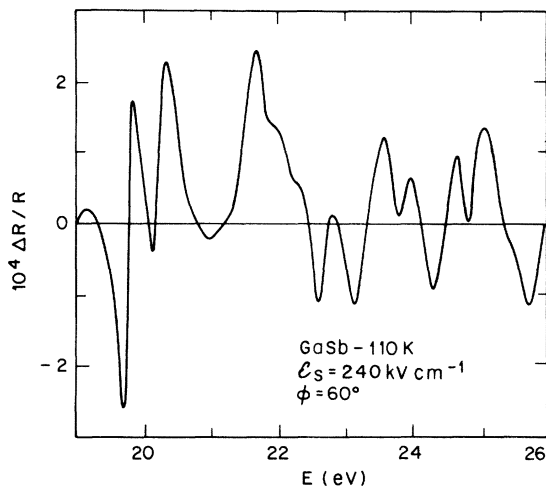


FIG. 8. Schottky barrier ER spectrum of transitions from the Ga $3d$ core valence bands in GaSb.

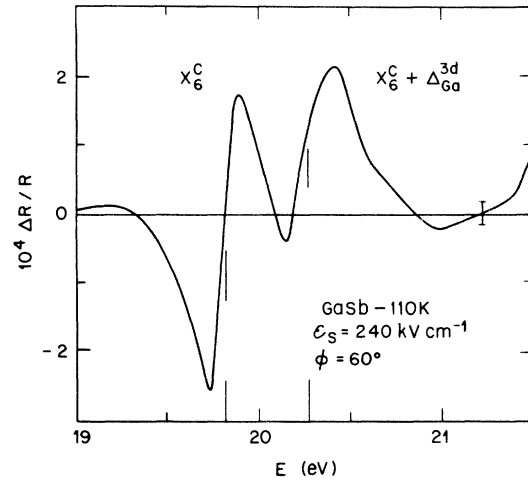


FIG. 9. Schottky barrier ER spectrum of the Ga $3d^V - X_6^C$ conduction-band critical points.

perimentally attainable energy range.

A detailed analysis of the Ga $3d^V - X_6^C$ transitions places the respective critical points at 19.82 ± 0.05 and 20.27 ± 0.05 eV, giving a spin-orbit splitting $\Delta_{Ga}^{3d} = 0.45 \pm 0.05$ eV which agrees with that previously obtained for GaAs and GaP,²⁰ and also for GaSe.⁶⁰ The strong feature that appears 1.8 eV above X_6^C in both GaAs and GaP should be present near 21.6 eV in Fig. 8, but it seems to be extremely weak or absent altogether. Some evidence for the strong feature 3.0 eV above X_6^C in GaAs and GaP is seen at 22.7 eV, or 2.9 eV above X_6^C in GaSb. The region of the conduction band giving rise to the latter transition therefore will bear an energy relationship to X_6^C that is essentially independent of the potential of the anion.

IV. DISCUSSION

The Schottky barrier ER spectra presented here contain a number of critical-point structures not previously observed. Some of these can be assigned, but others will require polarization measurements and more accurate band-structure calculations for their identification. To assist these calculations, more accurate critical-point energies are obtained for all higher-interband transitions for which positive identification can be made.

The band-structure calculation of Cahn and Cohen,⁸ probably the best currently available for GaSb, predicts a number of critical-point energies that are given in Table I. The most serious discrepancies occur over 4 eV. As Cahn and Cohen point out⁸ they were unable to remedy these discrepancies without causing unacceptable modifications of the lower-energy band structure within the local pseudopotential approximation, showing

TABLE I. Energies of selected high-symmetry critical points of GaSb. The experimental values are determined from Schottky barrier ER data unless otherwise referenced. The theoretical values are from a local pseudopotential band-structure calculation by Cahn and Cohen (Ref. 8).

Transition	Experiment	Theory ^a
$E_0 (\Gamma_8^V \rightarrow \Gamma_6^C)$	0.8102 eV ^b	0.9 eV
$E_0 + \Delta_0 (\Gamma_7^V \rightarrow \Gamma_6^C)$	1.559 ^c	1.7
$E_1 (L_6^V \rightarrow L_6^C)$	2.195 ± 0.010	1.93
$E_1 + \Delta_1 (L_{4,5}^V \rightarrow L_6^C)$	2.625 ± 0.010	2.43
$E_0' (\Gamma_8^V \rightarrow \Gamma_7^C)$	3.191 ± 0.005	
$E_0' + \Delta_0' (\Gamma_8^V \rightarrow \Gamma_6^C)$	3.404 ± 0.010	
$E_0' + \Delta_0' + \Delta_0'' (\Gamma_7^V \rightarrow \Gamma_6^C)$	4.160 ± 0.02	
$E_2(1) (\frac{3}{2}, \frac{1}{2}, \frac{1}{2}) (?)$	4.36 ± 0.03	} 3.9
$E_2(2) (\frac{3}{2}, \frac{1}{2}, \frac{1}{2}) (?)$	4.40 ± 0.03	
$E_2(3) (?)$	4.72 ± 0.05	
$X_7^V \rightarrow X_6^C (?)$	4.25 ± 0.1	
(?)	4.61 ± 0.05	
(?)	4.74 ± 0.05	
(?)	5.10 ± 0.03	
(?)	5.20 ± 0.05	
(?)	5.37 ± 0.03	
$E_1' \left\{ \begin{array}{l} (L_6^V \rightarrow L_{4,5}^C) \\ (L_6^V \rightarrow L_6^C) \end{array} \right.$	5.46 ± 0.02	
	5.59 ± 0.03	
$E_0'' \left\{ \begin{array}{l} (L_{4,5}^V \rightarrow L_{4,5}^C) \\ (L_{4,5}^V \rightarrow L_6^C) \end{array} \right.$	5.90 ± 0.07	
	6.04 ± 0.03	
(?)	6.9 ± 0.1	
$E_0'' (\Gamma_8^V \rightarrow \Gamma_{12}^C)$	7.9 ± 0.1	
(Ga $3d_{5/2} \rightarrow X_6^C$)	19.82 ± 0.05	
(Ga $3d_{3/2} \rightarrow X_6^C$)	20.27 ± 0.05	
$(\Gamma_6^C \rightarrow X_6^C)$ (indirect)	0.43 ± 0.2	0.48

^a Reference 8.

^b Reference 33.

^c From Ref. 33 with Δ_0 value from Reine *et al.*, Ref. 34.

that it is not adequate for the description of GaSb.

Much better agreement is obtained with the spin-orbit-splitting calculations of Wepfer *et al.*¹³ This is not surprising since the spin-orbit splittings depend more heavily on the atomic core potentials and are less influenced by crystal-field effects. Nevertheless, there are some discrepancies, notably in Δ_0 and in Δ_1 . The splitting $\Delta_0' = 213 \pm 10$ meV is remarkably small, being close to the value found in Ge ($\Delta_0' = 200 \pm 3$ meV)⁶ and in GaAs ($\Delta_1 = 171 \pm 15$ meV).⁷ This suggests that it is almost entirely due to the spin-orbit splitting of the cation.

TABLE II. Spin-orbit splittings at selected high-symmetry critical points of GaSb. The experimental values are determined from Schottky barrier ER data unless otherwise referenced. The theoretical values are from Wepfer, Collins, and Euwema (Ref. 13), calculated using the Kohn-Sham-Gaspar exchange.

Spin-orbit splitting	Experimental	Theoretical ^a
$\Delta_0 (\Gamma_8^V - \Gamma_7^V)$	749 meV ^b	} 660 meV
Δ_0 (from E_0' triplet)	756 ± 15	
$\Delta_0' (\Gamma_8^C - \Gamma_6^C)$	213 ± 10	260
$\Delta_1 (L_6^V - L_{4,5}^V)$	430 ± 10	} 390
Δ_1 (from E_1' transitions)	450 ± 30 (?)	
$\Delta_1' (L_6^C - L_4^C)$	130	140
$\Delta_2 (X_6^V - X_7^V)$	(?)	240
$\Delta_{3d}^{Ga} [(j = \frac{5}{2}) - (j = \frac{3}{2})]$	450 ± 50	460

^a Reference 13.

^b Reference 34.

It is interesting that the calculated spin-orbit splitting of the Ga $3d$ core state agrees almost exactly with experiment.

Our lower limit of 4.25 ± 0.1 eV for the $X_7^V - X_6^C$ critical point can be used with the pressure determination of the $\Gamma_1^C - X_6^C$ separation, 0.315 ± 0.015 eV,¹⁵ to place an upper limit on the energy of X_7^V . We note first that, although the pressure measurements were performed at room temperature and relevant ER measurements performed near liquid He temperature, the observed rigidity of the valence bands with temperature⁶¹ together with the near equality of the temperature coefficients of⁶¹ the E_0 and⁴⁸ E_2 structures insures that no essential difference occurs in the $\Gamma_1^C - X_6^C$ splitting as the temperature is changed. Thus we find X_7^V must lie at least $(4.25 \pm 0.1 \text{ eV}) - (0.810 \text{ eV}) - (0.32 \text{ eV}) = 3.1 \pm 0.1$ eV below Γ_8^V .

Structure assigned to X_5^V (average of X_6^V and X_7^V) has been observed in XPS measurements¹⁴ at -2.7 eV. Using the calculated spin-orbit splitting, $\Delta_2 = 0.24$ eV,¹³ we find that the XPS value of the energy of X_7^V relative to Γ_8^V is -2.6 eV. Thus our "best" value for X_7^V lies 0.5 eV deeper than that obtained from XPS data, which in turn agrees with local pseudopotential predictions for most III-V materials where calculations are available. But we believe that our value should be in better agreement with the results of nonlocal pseudopotential calculations, since one of the effects of the nonlocal pseudopotential is to spread the total width of the valence band. Specifically for Ge [the only material for which published data for X_4^V (or X_5^V) are available], the nonlocal pseudopotential increases the $X_4^V - \Gamma_{25}^V$ separation from 2.4 to 3.2 eV.² By analogy, one may anticipate a lowering of X_7^V , which should bring it into good agreement with the ER results.

Finally, we estimate the exciton binding energy between the Ga $3d^V$ valence band and the X_6^C relative minimum of the conduction band. XPS results locate Ga $3d^V$ at¹⁴ -19.00 ± 0.15 eV relative to Γ_8^V . Assuming the same relative shift between Γ_8^V and $3d_{5/2}^V$ as measured for GaP,⁶² we convert this value to low temperature by adding 0.02 eV. The $j = \frac{5}{2}$ level lies $\frac{2}{5}(0.45 \text{ eV}) = 0.18$ eV above this. Our measured Ga $3d_{5/2}^V - X_6^C$ separation of 19.82 eV therefore locates the X_6^C singularity (the core level $n = 1$ exciton line in the case of a sizeable interaction) at 1.02 ± 0.25 eV. The X_6^C energy can also be calculated by adding the E_0 gap at 110 K, 0.80 eV,⁶¹ to the $\Gamma_6^C - X_6^V$ splitting, 0.31 eV.¹⁵ We find $X_6^C = 1.11$ eV. The difference, 90 ± 250 meV, is

the exciton binding energy of the core level. This is of the order of that previously measured for GaP and GaAs.²⁰

ACKNOWLEDGMENTS

One of us (D.E.A.) wishes to acknowledge useful discussions with E. O. Kane. We also express our appreciation to A. A. Studna and A. Pisarchik for their assistance in preparing the samples used in these measurements. We have also benefitted from the cooperation of E. M. Rowe and the Synchrotron Radiation Center Staff. The Synchrotron Radiation Center was supported by the NSF under grant No. DMR-74-15089.

-
- ¹J. C. Phillips and K. C. Pandey, Phys. Rev. Lett. **30**, 787 (1973).
²K. C. Pandey and J. C. Phillips, Phys. Rev. B **9**, 1552 (1974).
³J. R. Chelikowsky and M. L. Cohen, Phys. Rev. Lett. **31**, 1582 (1973).
⁴J. R. Chelikowsky and M. L. Cohen, Phys. Rev. Lett. **32**, 674 (1974).
⁵W. D. Grobman and D. E. Eastman, Phys. Rev. Lett. **33**, 1034 (1974); W. D. Grobman, D. E. Eastman, and J. L. Freeouf, Phys. Rev. B **12**, 4405 (1975).
⁶D. E. Aspnes, Phys. Rev. Lett. **28**, 913 (1972).
⁷D. E. Aspnes and A. A. Studna, Phys. Rev. B **7**, 4605 (1973).
⁸R. C. Cahn and M. L. Cohen, Phys. Rev. B **1**, 2569 (1970).
⁹M. L. Cohen and T. K. Bergstresser, Phys. Rev. **141**, 789 (1966).
¹⁰F. Herman, R. L. Kortum, C. D. Kuglin, and J. P. Van Dyke, in *Methods in Computational Physics*, edited by B. Alder, S. Fernback, and M. Rotenberg (Academic, New York, 1968), Vol. 8, p. 193.
¹¹C. W. Higginbotham, F. H. Pollak, and M. Cardona, in *Proceedings of the Ninth International Conference on the Physics of Semiconductors* (Nauka, Leningrad, 1968), p. 57.
¹²H. I. Zhang and J. Callaway, Phys. Rev. **181**, 1163 (1969).
¹³G. G. Wepfer, T. C. Collins, and R. N. Euwema, Phys. Rev. B **4**, 1296 (1971).
¹⁴L. Ley, R. A. Pollak, F. R. McFeely, S. P. Kowalczyk, and D. A. Shirley, Phys. Rev. B **9**, 600 (1974).
¹⁵B. B. Kosicki, A. Jayaraman, and W. Paul, Phys. Rev. **172**, 764 (1968).
¹⁶D. L. Rode, B. Schwartz, and J. V. DiLorenzo, Solid-State Electron. **17**, 1119 (1974).
¹⁷A. A. Studna, Rev. Sci. Instrum. **46**, 735 (1975).
¹⁸C. G. Olson, M. Piacentini, and D. W. Lynch, Phys. Rev. Lett. **33**, 644 (1974).
¹⁹C. G. Olson and D. W. Lynch, Phys. Rev. B **9**, 3159 (1974).
²⁰D. E. Aspnes, C. G. Olson, and D. W. Lynch, Phys. Rev. B **12**, 2527 (1975).
²¹D. E. Aspnes, C. G. Olson, and D. W. Lynch, J. Appl. Phys. **47**, 602 (1976).
²²M. Haas and B. W. Hennis, J. Phys. Chem. Solids **23**, 1099 (1962).
²³D. E. Aspnes, Phys. Rev. B **15**, 4228 (1974).
²⁴D. E. Aspnes, Phys. Rev. Lett. **31**, 230 (1973).
²⁵P. Lawaetz, Phys. Rev. B **4**, 3460 (1971).
²⁶D. E. Aspnes, Phys. Rev. B **12**, 2297 (1975).
²⁷D. E. Aspnes, Surf. Sci. **37**, 418 (1973).
²⁸D. E. Aspnes and A. Frova, Solid State Commun. **7**, 155 (1969).
²⁹D. E. Aspnes and J. E. Rowe, Solid State Commun. **8**, 1145 (1970); Phys. Rev. B **5**, 4022 (1972).
³⁰D. E. Aspnes and J. E. Rowe, Phys. Rev. Lett. **27**, 188 (1971).
³¹E. J. Johnson and H. Y. Fan, Phys. Rev. **139**, A1991 (1965).
³²M. Reine, R. L. Aggarwal, and B. Lax, Phys. Rev. B **5**, 3033 (1972).
³³M. Reine, Ph.D. thesis (Massachusetts Institute of Technology, 1970) (unpublished), cited in Ref. 32.
³⁴M. Reine, R. L. Aggarwal, and B. Lax, Solid State Commun. **8**, 35 (1970).
³⁵D. D. Sell, S. E. Stokowski, R. Dingle, and J. V. DiLorenzo, Phys. Rev. B **7**, 4568 (1973).
³⁶D. E. Aspnes, J. Opt. Soc. Am. **63**, 1380 (1973).
³⁷J. E. Rowe and D. E. Aspnes, Phys. Rev. Lett. **25**, 162 (1970).
³⁸R. Enderlein, in *Proceedings of the Twelfth International Conference on the Physics of Semiconductors*, edited by M. Pilkuhn (Teubner, Stuttgart, 1974), p. 161.
³⁹R. Enderlein, P. Renner, and M. Scheele, Phys. Status Solidi B **71**, 503 (1975).
⁴⁰N. Bottka, R. Glosser, and J. Kinoshita, Bull. Am. Phys. Soc. **20**, 287 (1975).
⁴¹R. Glosser and B. O. Seraphin, Phys. Rev. **187**, 1021 (1969).
⁴²R. Glosser, J. E. Fischer, and B. O. Seraphin, Phys. Rev. B **1**, 1607 (1970).
⁴³N. Bottka and D. L. Johnson, Phys. Rev. B **11**, 2969 (1975).
⁴⁴T. Tuomi, M. Cardona, and F. H. Pollak, Phys. Status Solidi **40**, 227 (1970).
⁴⁵A. Iller, E. Kierzek-Pecold, and Z. Werfel, Acta Phys. Pol. A **43**, 55 (1973).

- ⁴⁶C. Alibert and G. Bordure, *Phys. Status Solidi* 40, 687 (1970).
- ⁴⁷L. M. Roth and B. Lax, *Phys. Rev. Lett.* 3, 217 (1959).
- ⁴⁸R. R. L. Zucca and Y. R. Shen, *Phys. Rev. B* 1, 2668 (1970).
- ⁴⁹M. Welkowsky and R. Braunstein, *Phys. Rev. B* 5, 497 (1972).
- ⁵⁰M. Cardona, K. Shaklee, and F. H. Pollak, *Phys. Rev.* 154, 696 (1967).
- ⁵¹J. C. Phillips, in *Solid State Physics*, edited by F. Seitz and D. Turnbull (Academic, New York, 1966), Vol. 18, p. 55.
- ⁵²T. M. Donovan, J. E. Fischer, J. Matsuzaki, and W. E. Spicer, *Phys. Rev. B* 3, 4292 (1971).
- ⁵³D. D. Sell and E. O. Kane, *Phys. Rev. B* 5, 417 (1972).
- ⁵⁴B. J. Parsons and H. Piller, *Solid State Commun.* 9, 767 (1971).
- ⁵⁵J. A. Van Vechten, *Phys. Rev.* 187, 1007 (1969).
- ⁵⁶F. H. Pollak, M. Cardona, C. W. Higginbotham, F. Herman, and J. P. Van Dyke, *Phys. Rev. B* 2, 352 (1970).
- ⁵⁷J. P. Walter and M. L. Cohen, *Phys. Rev.* 183, 763 (1969).
- ⁵⁸G. Guizzetti, L. Nosenzo, E. Reguzzoni, and G. Samoglia, *Phys. Rev. B* 9, 640 (1974).
- ⁵⁹K. C. Pandey and J. C. Phillips, *Phys. Rev. B* 9, 1560 (1974).
- ⁶⁰P. Thiry, R. Pincheaux, D. Dagneaux, and Y. Petroff, in *Proceedings of the Twelfth International Conference on the Physics of Semiconductors*, edited by M. Pilkuhn (Teubner, Stuttgart, 1974), p. 1275.
- ⁶¹D. Auvergne, J. Camassel, H. Mathieu, and M. Cardona, *Phys. Rev. B* 9, 5168 (1974).
- ⁶²D. E. Aspnes, C. G. Olson, and D. W. Lynch, *Phys. Rev. B* 14, 2534 (1976).